Journal of Applied Physics

Cathodoluminescence study of electric field induced migration of defects in single crystal *m*-plane ZnO

Jedsada Manyam,[1,a)] Cuong Ton-That,[2] and Matthew R. Phillips[2]

[1]*National Nanotechnology Center (NANOTEC), National Science and Technology Development Agency (NSTDA), Pathum Thani 12120, Thailand*

[2]*School of Mathematical and Physical Sciences, University of Technology Sydney, PO Box 123, Broadway, NSW 2007, Australia*

Internal electric fields can have a significant effect on the behavior of charged defects, dopants and impurities in operating electronic devices that can adversely impact on their long-term performance and reliability. In this paper, we investigate the redistribution of charged centers in single crystal m-plane ZnO under the action of a DC electric field at 873 K using in-plane and in-depth spatially resolved cathodoluminescence (CL) spectroscopy. The CL intensities of the ultra-violet near band edge (NBE) emission at 3.28 eV and green luminescence (GL) at 2.39 eV were observed to both uniformly increase on the anode side of the electrode gap. Conversely, towards the cathode the NBE and the GL steadily decrease and increase, respectively. The GL quenched after hydrogen donor doping confirming that the emission is related to acceptor-like centers. Based on the electro-migration and hydrogen doping results, the GL is attributed to radiative recombination involving Zn_i and V_{Zn} pairs. The intensity of an orange luminescence (OL) centered at 2.01 eV was unaffected by the electric field and is assigned to substitutional Li acceptors.

[a)] Electronic mail: jedsada@nanotec.or.th

I. INTRODUCTION

Point defects, such as vacancies, interstitials, and impurities, are inherently present in ZnO single crystals and nanostructures. These centers exist in neutral as well as singly or doubly ionized states, where the stable charge state for each defect is determined by the position of the Fermi level relative to their specific charge transition levels.[1] The presence of charged defects can have a significant impact on the stable operation and long term deterioration of ZnO-based electronic devices due to the electric field induced electro-migration effects.[2,3] For example, the underlying mechanism responsible for repetitively regulating electron conduction in ZnO resistive switching devices has been attributed to the electro-migration of oxygen ions (O^{2-}) and vacancies (V_O^{2+}) in the active layer.[4,5] Additionally, the diffusion of zinc interstitials (Zn_i^{2+}) and its complexes, such as $V_O^0 - Zn_i^{2+}$, into the grain boundaries of sintered ZnO varistors is believed to degrade the Schottky barrier and cause premature aging of these devices.[3] The physical origin and effects of defect migration in semiconductor devices and materials has been investigated using numerous experimental techniques, such as the pulsed electroacoustic (PEA) method,[6] deep level transient spectroscopy (DLTS),[7] photoluminescence (PL)[8] and transmission electron microscopy (TEM).[9] However, it should be emphasized that the unequivocal identification of defects in ZnO remains controversial. Uncertainty in the defect assignment can arise because different types of defects often affect the physical properties of ZnO in a similar way. Additionally, the presence of defect complexes can often complicate the interpretation of experimental results.[10]

Previous studies have reported changes to the spatial distribution and intensity of a green-colored emission in electric-field stressed ZnO devices and confirmed that the observed luminescence is related to mobile defects.[8,11,12] However, there is currently no consensus on the chemical identity of the mobile defect, which has been contradictorily attributed to both Zn interstitials (Zn_i)[8] and oxygen vacancy (V_O) - related defects.[11,12] A ubiquitous green

luminescence (GL) band in bulk and nanostructured ZnO is commonly observed as a broad structureless peak between 2.2 and 2.5 eV. The reported shift in the GL peak position is widely attributed to the presence of several highly overlapped broad emission peaks originating from a number of different defects or defect-related complexes.[10] The origin of GL emission has been ambiguously assigned to a very large number of different native point defects, impurities and complexes. However, due to their relative abundance and relatively low formation energies,[1,13] there is general agreement that the most likely candidates for the GL are either, V_O,[14-17] Zn vacancies (V_{Zn}),[16-20] and Zn_i[13] defects. According to Klason *et al*., annealing bulk ZnO in Zn-rich conditions generated V_O and resulted in a GL peak at 2.5 eV.[17] Conversely, heat treatment under O-rich conditions produced V_{Zn} and a GL peak at 2.35 eV. Ton-That *et al*.[17] reported that the GL in Zn-rich and O-rich ZnO exhibited a different response to H donor doping, confirming the presence of two peaks in the green spectral range. Furthermore, H annealing was found to quench the 2.35 eV peak, verifying that this O-rich GL is related to an acceptor-like Zn vacancy related defect.[18] Additionally, Korsunska *et al.*[21] reported an inhomogeneous GL intensity along a needle-shaped ZnO single crystal when subjected to DC biasing and suggested that a Zn_i complex may be involved in the GL.

In this work, we have used in-plane and in-depth cathodoluminescence (CL) microscopy and spectroscopy to investigate electric field-assisted migration of luminescence centers in the non-polar m-plane ($10\underline{1}0$) ZnO single crystals. Here, we aim to gain greater insight into the behavior of charged defects in ZnO when subjected to an electric field at elevated temperature. We report CL characterization of the defect distribution on the surface of hydrothermally grown ZnO single crystal before and after the application of an electric field at 873 K. Our results support the assignment of the GL to radiative recombination involving ($Zn_i - V_{Zn}$) pairs and the OL to substitutional Li acceptors.

II. EXPERIMENTAL DETAILS

A $5 \times 4\ mm^2$ sample was cut from a hydrothermally grown, $10 \times 10 \times 0.5\ mm^3$, polished both sides, *m*-plane n-type ZnO single crystal substrate supplied by MTI Corporation (CA, USA). Two $1.5 \times 2.5\ mm^2$ Ti (50 nm) / Au (30 nm) electrodes with a gap of 0.4 mm were deposited on the (10$\underline{1}$0) face of the ZnO sample using DC magnetron sputtering. I-V curves were measured using a Yokogawa GS610 source and measurement unit (SMU). Before conducting the electro-migration experiments the samples were cleaned with ethanol in an ultrasonic bath and rinsed with deionized water, and subsequently annealed in a horizontal quartz tube furnace at 873 K in argon (oxygen-poor) with a flow rate of 10 sccm for 3 hours. The pre-annealing treatment of the ZnO sample was done to stabilize the ZnO defect structure at 873 K and ensure that the observed thermally assisted electro-migration induced changes were due predominately to the effect of the electric field. Electric field-assisted migration experiments were conducted at 873 K in argon with a flow rate of 10 sccm for 3 hours using a DC bias of 30 volts across the Ti / Au, which produced an electric field strength of ~ 750 V/cm. The sample was allowed to cool down with the bias on to room temperature without assistance before being removed from the furnace. Hydrogen donors were incorporated into an additional $5 \times 4\ mm^2$ sample cut from the original MTI ZnO substrate using a radio-frequency hydrogen plasma with the power of 15 W at 473 K for 10 minutes.

CL measurements were performed using a FEI Quanta 200 scanning electron microscope equipped with a Gatan C1002 liquid nitrogen cold stage and an Ocean Optics QE65000 spectrometer. A typical CL spectrum was collected from a scan area of $15 \times 20\ \mu m^2$ with accelerating voltage of 10 kV and beam current of 1 nA at room temperature or 0.1 nA at 85 K. To observe electric field induced migration of luminescent centers, CL spectra were collected before and after the electro-migration experiment (describe above) from 7 positions between two electrodes as illustrated in Fig. 1(a). Depth-resolved CL (DRCL) measurements

were performed to probe the spatial distribution of luminescence centers as a function of depth from the surface of the sample. Here, CL spectra were collected between two electrodes at 85 K with accelerating voltages varied between 5 kV and 30 kV, corresponding to CL probing depths ranging between approximately 100 and 1800 nm, respectively: These values represent depths at which 70% of the electron energy loss has occurred using CASINO Monte Carlo simulation methods.[22] An equivalent electron-hole pair generation rate was used at each kV by using adjusting the electron beam current to provide a constant electron beam power of 1 μW.

III. RESULTS AND DISCUSSION

A. CL Characterization of ZnO

Typical CL spectra at 85 K of the "as received" annealed ZnO at 873 K (henceforth referred to as sample A), hydrogen doped sample A, and post-hydrogen-doped annealed at 573 K samples collected at the same excitation conditions (10 kV and 0.1 nA) are shown in Fig. 2(a). Sample A exhibits a near band edge (NBE) with two sharp peaks located at 3.36 eV and 3.25 eV and a broad deep-level emission (DLE) band in green-yellow spectral region centered at 2.3 eV. The higher energy NBE peak is due to donor bound exciton (DBX) *I* – lines, while the second NBE peak is consistent with longitudinal optical (LO) phonon replica emission of the free exciton (FX), which have an energy spacing of 72 meV in ZnO.[23] The presence of the LO phonon replicas confirms the high crystalline quality of sample A. The broad structureless DLE band at 85 K arises from the presence of two broad, defect-related emission bands that are highly overlapped, containing a green luminescence (GL) and an orange luminescence (OL) peaks, centered at ~ 2.39 eV and ~ 2.01 eV, respectively.

Following H incorporation in sample A, the NBE intensity increased fourfold and the higher energy GL defect luminescence peak was completely absent, leaving a single OL peak located at 2.01 eV, as shown in Fig. 2(a). The increased NBE emission is due to a higher concentration of hydrogen-related I_4 donor-bound excitons[17,23] and, most likely, the removal

of a non-radiative recombination channel that acts as a competitive recombination pathway to the NBE luminescence. As the NBE and DLE are also competitive recombination pathways, the higher NBE recombination reduces the DLE intensity. The strong quenching of the GL is attributed to a hydrogen passivation mechanism. Since H is stable as a positive donor in ZnO, it can interact strongly with negatively charged acceptor-like defects. Accordingly, as V_{Zn} acceptors have the lowest formation energy in n-type ZnO,[1] the GL is attributed to an ionized Zn vacancy-related center as reported elsewhere in the literature, which is quenched by H passivation.[16,17,24] This model is strongly supported by the recovery of the GL after H is removed by re-heating the sample to 573 K for 10 minutes in argon as illustrated in Fig. 2(a). The chemical identity of the OL at 2.01 eV is also controversial for being assigned to oxygen interstitials (O_i)[25] as well as transitions involving Li acceptors.[26] However, as recent work has contradicted the O_i assignment[27] and as Li is definitely present in our samples as due to the use of a LiOH mineralizer that facilitates hydrothermal growth,[28,29] the OL at 300 K is attributed to a transition involving substitutional Li impurities on Zn sites. In the process, negative Li_{Zn}^{-} ions trap excited free holes forming neutral Li_{Zn}^{0} centers that relax to their original ionized state by capturing an excited free electron and emitting the observed OL.

A typical CL spectrum (10 kV and 1 nA) at room temperature of sample A is shown in Fig. 2(b). At 300 K, the DBX emission is quenched as a result of thermal ionization and the NBE is dominated by a peak at around 3.28 eV arising from the highly overlapped emission of FX phonon replicas that are of red-shifted and broadened due to thermal lattice expansion and the electron-phonon effect. The dominance of the GL in Fig. 2(b) suggests that the OL has saturated with the higher 1 nA excitation current which is consistent with the reported long relaxation time of the OL.[30] The Gaussian peak fitting depicted in Fig. 2(c) of the broad DLE at 300 K shown in Fig. 2(a) reveals that the energy position and FWHM of the GL and OL

emission peak are at 2.39 eV (FWHM = 0.51 eV) and 2.01 eV (FWHM = 0.52 eV), respectively.

B. Electron-migration experiment

Electrical current vs voltage (I-V) measurements (Fig. 1(b)) revealed that the resistance of the "as received" MTI ZnO substrate was approximately 10 kΩ, which increased to ~ 1 MΩ in sample A, and the value was in the order of kΩ at 873 K. The 100× increase in the resistance of sample A after annealing is due to the out-diffusion of interstitial Li donors, Li_i, that are inadvertently incorporated during hydrothermal growth.[31]

To investigate defect electro-migration in ZnO, a DC electric field was applied at the surface of sample A through parallel electrode pads, as shown in Fig. 1(a), while annealing at 873 K. The spatially-resolved CL characterization results of the thermally assisted electro-migration experiments are presented in Figs. 3(a) and 3(b). These data show a comparison of the NBE, OL and GL intensities from a series of identical positions spanning the surface between the electrodes before and after the electric field was applied at 873 K. The peak intensities were obtained from a set of CL spectra collected at separate locations in a straight line between two electrodes at 50 μm intervals, as shown by cross (×) marks in Fig. 1(a). Typical Gaussian peak fitted CL spectra prior to and following the application of the electric field are shown in Fig. 3(c). These data are collected from the location marked with an (o) in Fig. 1(a).

The CL intensity versus the electrode gap position plots in Figs. 3(a) and 3(b) reveal that on the positive electrode (anode) side both the NBE and GL uniformly increase intensity after application of the electric field and exhibit the same line shape profile as sample A. On the negative electrode (cathode) side of the gap, however, the GL and NBE intensities are observed to steadily increase and decrease, respectively, when moving towards the cathode.

Conversely, the OL intensity is constant across the entire gap between the electrodes and remained unchanged before and after the electro-migration experiment, as shown in Fig. 3(b).

Depth-resolved CL spectra were collected using accelerating voltages of 5, 10, 20 and 30 kV with a constant beam power of 1μW to reveal the effect of the electric field on the spatial distribution and concentration of defects in-depth. Figures 4(a) and 4(b) show the GL and OL intensities versus kV (depth) before (sample A) and after the electro-migration experiment, respectively, collected at near the cathode marked point A in Fig. 1(a). These plots show that the GL in-depth distribution increases moving towards the surface while the OL intensity profile is unaffected by the electric field in accordance with the in-plane results depicted in Figs. 3(a) and 3(b). The decrease in the GL and NBE at the very near surface at 5 kV strongly suggests the presence of enhanced non-radiative surface recombination after annealing in the electric field while the decrease of the NBE at 30 kV is due to internal optical absorption. The OL intensity steadily decreasing towards the surface in both Figs. 4(a) and 4(b) confirms the out-diffusion of Li following the pre-annealing of the as-received sample which causes the measured increase in the resistance of sample A.

A number of significant conclusions can be drawn from the experimental results described above. First, the uniform increase of both the NBE and GL intensity by the electric field on the anode side of the gap indicates that a defect that acts as a competitive non-radiative recombination channel has been passivated during the electro-migration experiment, most likely via the trapping of carriers driven across the gap by the action of the electric field. Notably, the OL intensity remains constant despite the passivation of the non-radiative channel suggesting that the capture cross-section of the OL defect may be smaller than that of the GL center. Second, charged defects are mobile during the thermally assisted electro-migration experiment. Third, the GL and NBE are confirmed as competitive recombination pathways, accordingly as the GL center concentration increases towards the negative electrode the NBE

intensity decreases, as observed in Figs. 3(a) and 3(b). Finally, since the OL intensity is unaffected by the application of the electric field at 873K, substitutional Li is considered to be immobile under these electro-migration conditions.

The change in the spatial distribution GL intensity after the electro-migration experiment results from either the electro-migration of positive defects towards or negative defects away from the cathode, respectively. In ZnO, candidates for positive defects include Zn_i^{2+}, V_O^{2+}, H_i^+, Li_i^+ as well as shallow donors e.g. Al_{Zn}^+, while for negative centers include V_{Zn}^{2-}, Li_{Zn}^-, and O_i^{2-}. The involvement of H_i^+ and Li_i^+ in the increase GL near the cathode can be ruled out due to their out-diffusion during the pre-annealing at 873 K, which was evidenced by our electrical and depth-resolved CL results. Similarly, V_{Zn}^{2-}, V_O^{2+}, and O_i^{2-} can be dismissed due to their high migration barrier energies of 1.4, 1.7 and 1.1 eV, respectively.[32] By the same argument, shallow donors, Al and Ga as well as Li_{Zn}^- are unlikely with their large diffusion activation energies of 2.7, 3.8 and 1.7 eV, respectively.[33,34]

Despite the relatively high formation energy of Zn_i^{2+} in oxygen-poor, n-type ZnO compared with V_{Zn}, V_O and O_i,[1] Zn_i^{2+}shallow donors must be present during the electro-migration experiment as evidenced by the high conductivity observed in the I-V measurement at 873 K. Furthermore, Zn_i^{2+} has a low migration barrier energy of 0.55 eV[34] and so will have a high mobility in ZnO.[35] However, Zn_i cannot be responsible for the GL at 2.39 eV by itself as it is a shallow donor with an ionization energy of 30 meV.[1] The results shown in Fig. 2(a) confirm that the GL is related to an acceptor-like defect because the GL is quenched by H donor doping and can be subsequently re-activated by thermal annealing at 573 K for 10 min, as described above. Therefore, the most likely candidate for the GL is V_{Zn}-related center as V_{Zn} acceptors have the lowest defect formation energy in oxygen-poor, n-type ZnO. Ascribing the GL to a negatively charged center is, however, inconsistent with the results of the electro-migration experiment which revealed an increase of the GL towards the negative electrode in

the electro-migration experiment. Additionally, V_{Zn} has a large high migration barrier energy (E_b = 1.4 eV) and can be considered to be immobile compared with Zn_i (E_b = 0.55 eV).[32,34]

Our electro-migration results strongly suggest that both Zn_i and V_{Zn} are involved in the GL emission process. This assignment is in agreement with other reports that have ascribed the GL to electron hole recombination transitions from spatially extended shallow Zn_i donor states to deep V_{Zn} localized acceptors.[36,37] Additionally, it has also been recently reported that GL is due to closely bound ($Zn_i - V_{Zn}$) pairs.[38] Therefore, in the electro-migration experiment, the GL intensity rises towards the cathode because of an increasing number of ($Zn_i - V_{Zn}$) pairs with overlapping wave functions, which form as positive Zn_i donors migrate to the negative electrode and interact with relatively immobile V_{Zn} acceptors. In contrast, the electric field independence of the OL center distribution in the electro-migration experiment can be explained by the poor mobility of substitutional Li in ZnO.[39,40]

IV. CONCLUSION

Spatially-resolved in-plane and in-depth CL spectra were measured before and after the application of a surface electric field at 873 K. The thermally assisted electro-migration experiment confirmed the migration Zn_i towards the cathode, inducing a steady decrease and increase of the NBE and GL, respectively. The GL at 2.39 eV is attributed to recombination involving ($Zn_i - V_{Zn}$) pairs and an OL at 2.01 eV, which is unaffected by the electric field, is assigned to substitutional Li acceptors. Significantly, following the electro-migration experiment the intensity of the NBE and GL was increased uniformly on the anode side of the electrode gap due to the passivation of competitive non-radiative recombination via the trapping of free carriers.

ACKNOWLEDGEMENTS

J.M. acknowledges the financial support from the Australian Endeavour research fellowship program, Australian Government. Financial support from the National Science and Technology Development Agency (NSTDA), Thailand, (Grant no. P1450015) is also acknowledged. The authors thank G. McCredie, M. Lockrey, L. Zhu and S. Choi for technical support.

REFERENCES

[1]A. Janotti and C. G. Van de Walle, Phys. Rev. B **76**, 165202 (2007).

[2]F. M. Simanjuntak, D. Panda, K.-H. Wei1, and T.-Y. Tseng, Nanoscale Res. Lett. **11**, 368 (2016).

[3]J. He, C. Cheng, and J. Hu, AIP Adv. **6**, 030701 (2016).

[4]A. Shih, W. Zhou, J. Qiu, H-J. Yang, S. Chen, Z. Mi, and I. Shih, Nanotechnology **21**(12), 125201 (2010).

[5]F. Pan, C. Chen, Z. Wang, Y. Yang, J. Yang, and F. Zeng, Prog. Nat. Sci.: Mater. Int. **20**, 1 (2010).

[6]C. Cheng, J. He, and J. Hu, Appl. Phys. Lett. **105**, 133508 (2014).

[7]A. Rohatgi, S. K. Pang, T. K. Gupta, and W. D. Straub, J. Appl. Phys. **63**(11), 5375 (1988).

[8]M. S. Ramanachalam, A. Rohatgi, W. B. Carter, J. P. Schaffer, and T. K. Gupta, J. Electron. Mater. **24**(4), 413 (1995).

[9]J.-Y. Chen, C.-L. Hsin, C.-W. Huang, C.-H. Chiu, Y.-T. Huang, S.-J. Lin, W.-W. Wu, and L.-J. Chen, Nano Lett. **13**(8), 3671 (2013).

[10]Ü. Özgür, Ya. I. Alivov, C. Liu, A. Teke, M. A. Reshchikov, S. Doğan, V. Avrutin, S.-J. Cho, and H. Morkoç, J. Appl. Phys. **98**, 041301 (2005).

[11]S. Tanaka, K. Takahashi, T. Sekiguchi, K. Sumino, and J. Tanaka, J. Appl. Phys. **77**(8), 4021 (1995).

[12]V. Sh. Yalishev, Y. S. Kim, B. H. Park, and Sh. U. Yuldashev, Appl. Phys. Lett. **99**, 012101 (2011).

[13]D. C. Look, J. W. Hemsky, and J. R. Sizelove, Phys. Rev. Lett. **82**, 2552 (1999); D. C. Look, G. C. Farlow, P. Reunchan, S. Limpijumnong, S. B. Zhang, and K. Nordlund, Phys. Rev. Lett. **95**, 225502 (2005).

[14]M. R. Phillips, O. Gelhausen, and E. Goldys, Phys. Status. Solidi. A **201**, 229 (2004).

[15]M. Foley, C. Ton-That, and M. R. Phillips, Appl Phys Lett. **93**, 243104 (2008).

[16]P. Klason, T. M. Borseth, Q. X. Zhao, B. G. Svensson, A. Y. Kuznetsov, P. J. Bergman, and M. Willander, Solid State Commun. **145**, 321 (2008).

[17]C. Ton-That, L. Weston, and M. R. Phillips, Phys. Rev. B **86**, 115205 (2012).

[18]L. Weston, C. Ton-That, and M. R. Phillips, J. Mater. Res. **27**(17), 2220 (2012).

[19]F. Fabbri, M. Villani, A. Catellani, A. Calzolari, G. Cicero, D. Calestani, G. Calestani, A. Zappettini, B Dierre, T. Sekiguchi, and G. Salviati, Sci. Rep. **4**, 5158 (2014).

[20]Z. Wang, S.C. Su, M. Younas, F.C.C. Ling, W. Anwand, and A. Wagner, RSC Adv. **5**, 12530 (2015).

[21]N. O. Korsunska, L. V. Borkovska, B. M. Bulakh, L. Y. Khomenkova, V. I. Kushnirenko, and I. V. Markevich, J. Lumin. **102-103**, 733 (2003).

[22]D. Drouin, A. Couture, D. Joly, X. Tastet, V. Aimez, and R. Gauvin, Scanning **29**(3), 92 (2007).

[23]B. K. Meyer, H. Alves, D. M. Hofmann, W. Kriegseis, D. Forster, F. Bertram, J. Christen, A. Hoffmann, M. Straßburg, M. Dworzak, U. Haboeck, and A. V. Rodina, Phys. Stat. Sol. (b) **241**(2), 231 (2004).

[24]L. L. C. Lem, C. Ton-That, and M. R. Phillips, J. Mater. Res. **26**(23), 2912 (2011); L. L. C. Lem, M. R. Phillips, and C. Ton-That, J. Lumin. **154**, 387 (2014).

[25]C. V. Manzano, D. Alegre, O. Caballero-Calero, B. Alén, and M. S. Martín-González, J. Appl. Phys. **110**, 043538 (2011).

[26]J.D. McNamara, N.M. Albarakati, and M.A. Reshchikov, J. Lumin. **178**, 301 (2016).

[27]J. Lv and M. Fang, Mater. Lett. **218**, 18 (2018).

[28]O. F. Schirmer and D. Zwingel, Solid State Commun. **8**(19), 1559 (1970).

[29]R.T. Cox, D. Block, A. Hervé, R. Picard, C. Santier, and R. Helbig, Solid State Commun. **25**, 77 (1978).

[30]M. A. Reshchikov, H. Morkoc, B. Nemeth, J. Nause, J. Xie, B. Hertog, and A. Osinsky, Physica B **401–402**, 358 (2007).

[31]E. D. Kolb and R. A. Laudise, J. Am. Ceram. Soc. **48**, 342 (1965); J. Am. Ceram. Soc. **49**, 302 (1966).

[32]A. Janotti and C. G. Van de Walle, Rep. Prog. Phys. **72**, 126501 (2009).

[33]V. J. Norman. Aust. J. Chem., **22**(2), 325 (1969).

[34]D. G. Thomas. J. Phys. Chem. Solids **3**(3–4), 229 (1957).

[35]P. Erhart and K. Albe, Appl. Phys. Lett. **88**, 201918 (2006).

[36]H. Chen, S. L. Gu, K. Tang, S. M. Zhu, Z. B. Zhu, J. D. Ye, R. Zhang, and Y. D. Zheng, J. Lumin. **131**(6), 1189 (2011).

[37]Z. R. Yao, S. L. Gu, K. Tang, J. D. Ye, Y. Zhang, S. M. Zhu, and Y. D. Zheng, J. Lumin. **161**, 293 (2015).

[38]K. Tang, R. Gu, S. Zhu, Z. Xu, and Z. Xu, Opt. Mater. Express **7**(4), 1169 (2017).

[39]K. E. Knutsen, K. M. Johansen, P. T. Neuvonen, B. G. Svensson, and A. Yu. Kuznetsov, J. Appl. Phys. **113**(2), 023702 (2013).

[40]G. Li, L. Yu, B. M. Hudak, Y.-J. Chang, H. Baek, A. Sundararajan, D. R. Strachan, G.-C. Yi, and B. S. Guiton, Mater. Res. Express **3**, 054001 (2016).

Figure captions

Fig. 1. (a) Top-view drawing of the sample showing ohmic electrode pads (gray) configuration on the *m*-plane ZnO surface. The lateral 10 kV CL measurement positions, marked with an (×) between the electrodes, were at 60 μm and 30 μm away from the positive and negative electrodes, respectively with a spacing of 50 μm. The depth-resolved CL measurement point was located 50 μm away from the negative electrode indicated by an (o). (b) I-V characteristic of the ZnO substrate measured between two electrodes, showing an ohmic resistance of approximately 10 kΩ. The measured resistance was in the order of kΩ during the application of DC bias at the elevated temperature.

Fig. 2. (a) Comparison of typical CL spectra at 85 K of an as-received annealed at 873 K (Sample A), hydrogen-doped sample A (H-doped), and post-annealed hydrogen doped sample A (post annealed at 573 K for 10 minutes in argon; H-doped annealed) hydrothermal m-plane ZnO samples before application of electric field, measured at the middle of the gap between two electrodes with 10 kV and 0.1 nA electron beam; Typical peak fitting parameters are fitting values are OL = 2.01 eV (FWHM = 0.52 eV) and GL = 2.39 eV (FWHM = 0.47 eV), (b) CL spectrum at 300 K of sample A excited with 10 kV and 1 nA electron beam; (c) Two Gaussian components, OL and GL at 300 K, fitted to a DLE band for sample A shown in Fig. 2 (b) with the OL component centered at 2.01 eV (FWHM = 0.52 eV) and GL component positioned at 2.39 eV (FWHM = 0.51 eV).

Fig. 3. Results of electro-migration experiments conducted on sample A using 30 V at 873 K in argon. Plots of the CL intensity versus distance from the positive electrode as marked by the (×) in Fig. 1(a) are shown in (a) for the NBE integrated peak intensity and in (b) for the OL and GL integrated peak intensities. Figure 3(c) shows the Gaussian fitted spectra before and after the application of DC bias at 873 K from the location marked (×) next to the negative electrode in Fig. 1(a). All CL spectra were measured at ~ 300 K using 10 kV and I_B = 1 nA. The peak fitting parameters are for the OL = 2.01 eV (FWHM = 0.52 eV) and for the GL = 2.40 eV (FWHM = 0.51 eV).

Fig. 4. Plots of the integrated peak intensity of OL and GL as a function of accelerating voltage of sample A (a) before and (b) after the electro-migration experiment measured at point (o), shown in Fig. 1(a). The depth-resolved CL spectra were collected at 85 K with an accelerating voltage of 5, 10, 20 and 30 kV and a constant beam power of 1 μW obtained by varying I_B. The inset in each Figs. shows the CL spectra labeled with OL and GL peak positions at varying accelerating voltages.

AIP Publishing

Journal of Applied Physics

ACCEPTED MANUSCRIPT

This is the author's peer reviewed, accepted manuscript. However, the online version of record will be different from this version once it has been copyedited and typeset.
PLEASE CITE THIS ARTICLE AS DOI: 10.1063/1.5134555

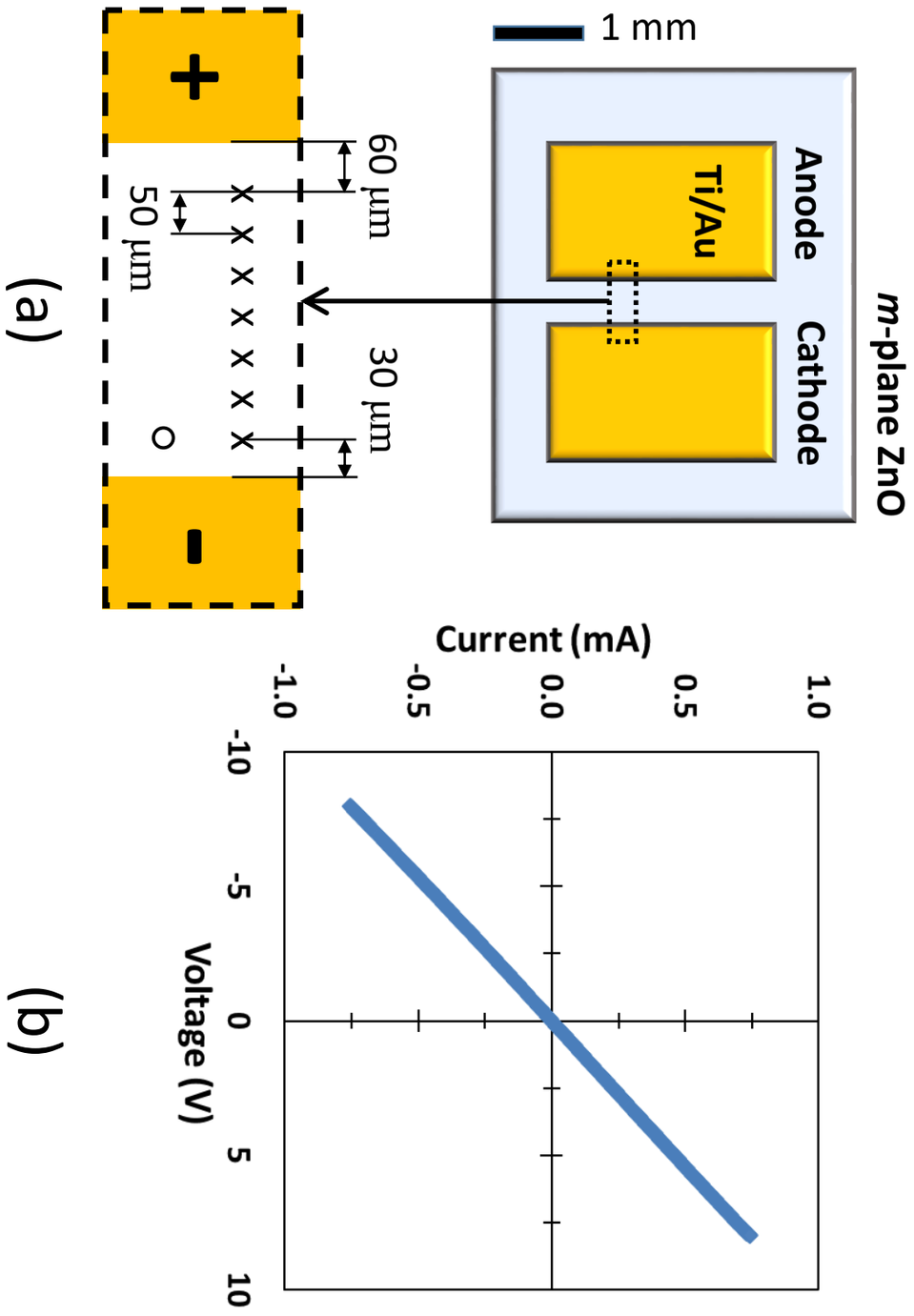

AIP Publishing
Journal of Applied Physics
ACCEPTED MANUSCRIPT

PLEASE CITE THIS ARTICLE AS DOI: 10.1063/1.5134555

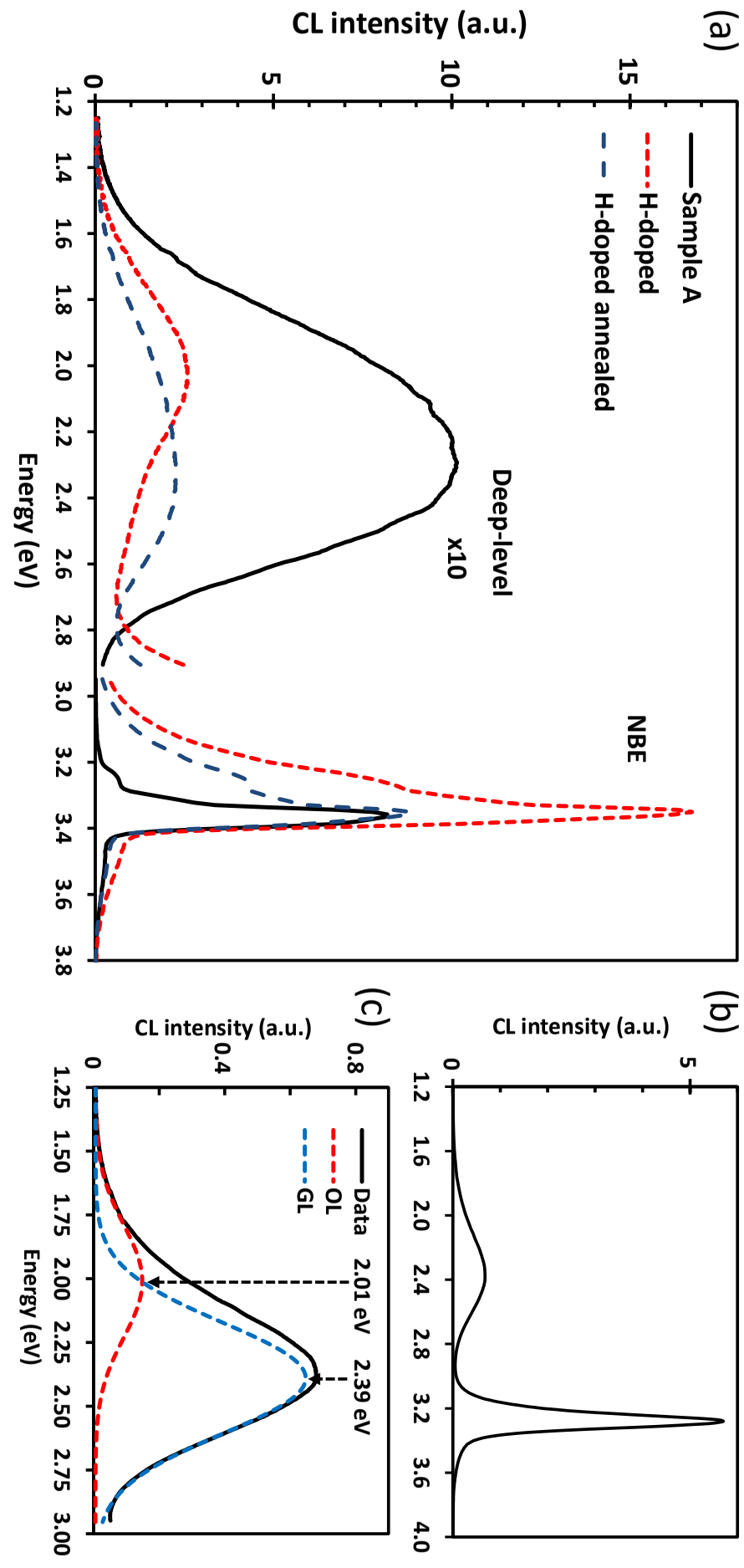

AIP Publishing

Journal of Applied Physics

ACCEPTED MANUSCRIPT

This is the author's peer reviewed, accepted manuscript. However, the online version of record will be different from this version once it has been copyedited and typeset.
PLEASE CITE THIS ARTICLE AS DOI: 10.1063/1.5134555

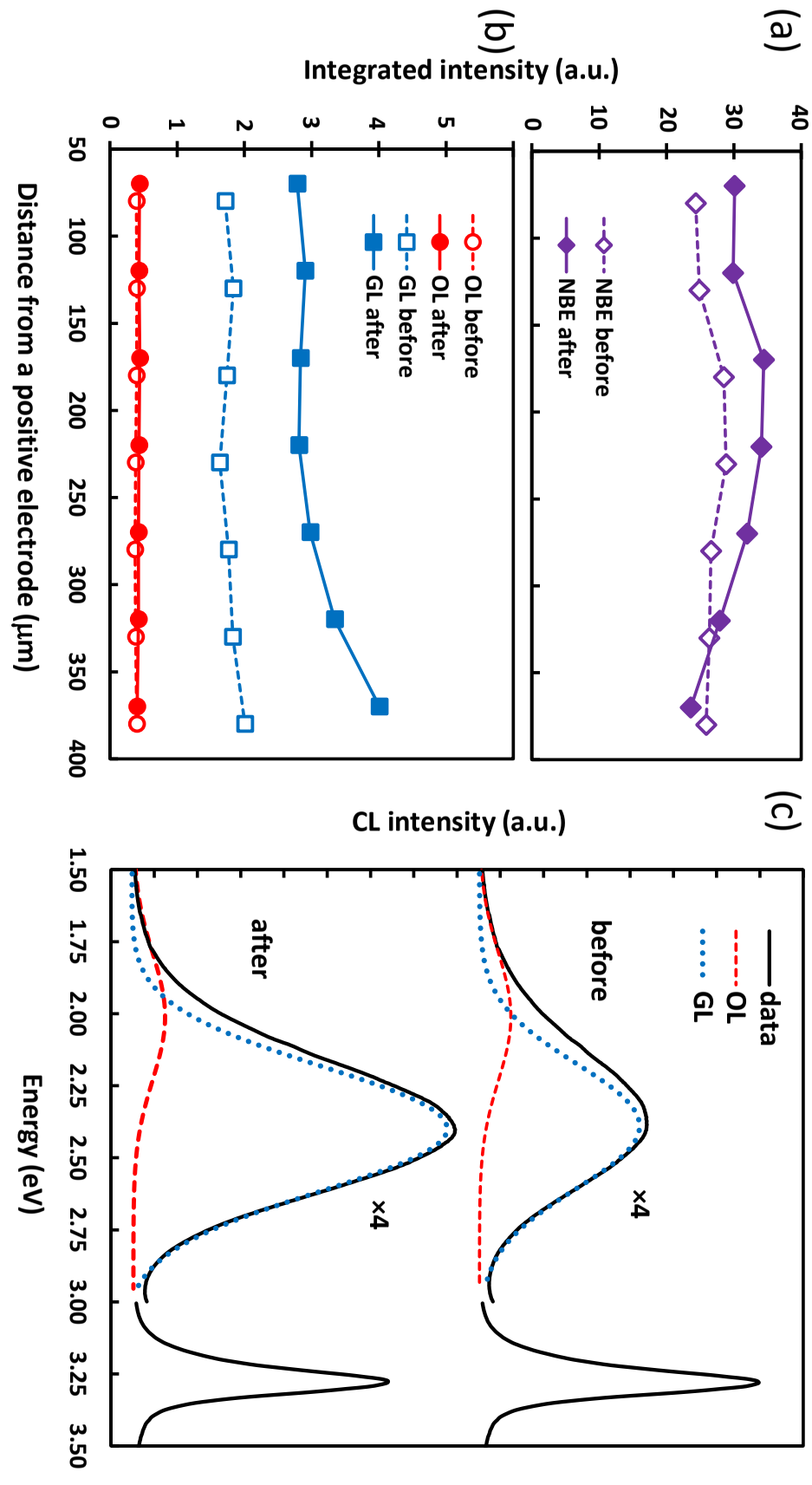

AIP Publishing

Journal of Applied Physics

ACCEPTED MANUSCRIPT

This is the author's peer reviewed, accepted manuscript. However, the online version of record will be different from this version once it has been copyedited and typeset.
PLEASE CITE THIS ARTICLE AS DOI: 10.1063/1.5134555